Numerical Investigation of Interaction between Saccular Abdominal Aortic Aneurysms and Arterial Bifurcations

Kadhum Audaa Jehhef[1*], Ali Jalal Ali[2]

[1] *Department of Machines and Equipment, Institute of Technology*
Middle Technical University
Muasker Al Rashid Street, Baghdad, Iraq
E-mail: kadhum.audaa@yahoo.com

[2]*Department of Biomedical Engineering*
University of Technology
Baghdad 10066, Iraq
E-mail: 10678@uotechnology.edu.iq

**Corresponding author*

Received: February 21, 2020 **Accepted: February 17, 2021**

Published: September 30, 2021

Abstract: *In order to fully understand the interaction between the Abdominal Aortic Aneurysms (AAAs) and the arterial bifurcations interface it is important to attain more detailed information on blood hemodynamics stresses by using an accurate and real model of the vascular system of the human. In this study, a computer simulation, which integrates dinically acquired of 73-year-old male patient with saccular AAA MR angiograms image is considered. The numerical predictions for 2D of two models (with and without saccular AAA) – axisymmetric, rigid wall Newtonian and non-Newtonian Carreau blood model are presented. The finite volume method performed by ANSYS-Fluent Package was used to model this problem. The blood hemodynamics is considered as steady state condition in two values of Reynolds numbers of laminar flow condition. Blood hemodynamics is calculated for an improved set of dimensionless values pointer parameters include the pressure dimensionless, dimensionless Wall Shear Stress (WSS) and flow velocity. The results show that at the turbulent flow, velocity is with highest fluctuation profile and generate some vortices near the inner wall of AAA. The highest WSS levels are obtained downstream of AAA and at bifurcation apex. The presence of AAA in flow path will increase blood velocity of the distal by 35% for laminar and about 42% for turbulent. Finally, the velocity profile was compared with previous literature and give good agreement at the same computational condition.*

Keywords: *Hemodynamics, Non-Newtonian blood, Blood heat transfer, AAA.*

Introduction

In the medical terminology, an Abdominal Aorta Aneurysm (AAA) means an abnormal, unrefined, enduring, localized dilatation at any section of the artery. The aneurysmal is an expansion that is greater than twice or more the normal size of the conventional artery diameter. The AAAs are distinguished into three foremost arrangements: Fusiform Abdominal Aorta Aneurysm (FAAA) where the enlargement is symmetrical about the central axis of the artery; Saccular Abdominal Aorta Aneurysm (SAAA), where the enlargement is at one artery side and Fusiform/Saccular Abdominal Aorta Aneurysm (FSAAA), where all artery sides are enlarged but are nonsymmetrical about the central axis of the artery. The diameter of the aneurysm is with four times by comparing with the artery normal diameter and it can expand by 0.2-1.0 cm/year till it unexpectedly ruptures [2]. Thus, the foremost difficulties with AAA that called the "silent killer" is that they are often asymptomatic till it ruptures [12]. Numerous

numerical and experimental revisions have surveyed the flow patterns and behaviours in the AAA by using both steady and pulsatile flow conditions. Altuwaijri [1] has experimentally found that the AAA reparation needs medical interference. Moreover, in patients with stable AAA, the surgery interaction has rate of mortality by 5%. Therefore, the blood flow behaviours inside the AAA can powerfully effect the distribution and magnitude of wholly blood flow apparatuses of the flow forces on the AAA wall [19]. Yu et al. [21] presented an experimental study of the hemodynamics of various AAA models by utilizing the Particle Image Velocimetry (PIV). They show that the upstream blood flow before the aneurysm region containing two portions: a major flow core crosswise of the pipe and a minor thin boundary layer that involved to the tube wall. Yu [20] has used PIV. Reynolds number is ranged from 400 to 1400 and Wimberley number is ranged from 17 to 22 for both pulsatile and steady blood flow conditions. The results show that when the flow condition is steady, there is a recirculating vortices engaged the whole rounded tube bulge, and the vortices core is located earlier to the end of the bulge distal. Moreover, Molla [14] performs a technique of Large Eddy Simulation (LES) to model the several kinds of pulsatile blood flow of the Newtonian and non-Newtonian fluid models. His results displayed that within the aneurysm region a large re-circulation vortex exists. Also, the mathematical expectations of hemodynamics stresses and blood flow configurations inside the AAAs are accomplished by Finol and Amon [5].

The Wall Shear Stress (WSS) are the lateral forces that acts on the walls of the AAA. Peattie et al. [15] has experimentally established a study of seven AAA models. The authors show that the WSS appeared as constant in tube upstream, quickly reduced in the tube bulge but it is amplified at the end of the distal of tube bulge due to the occurrence of the sharp velocity gradients. Some of the experimental and numerical data indicated that the maximum WSS was used as an enhanced forecaster of the AAA rupture than the AAA diameter. Speelman et al. [16] show that the WSS is significantly effect by AAA diameter, AAA shape, blood pressure, local curvature of aneurysm wall and thickness of the aneurysm wall. Also, Fillinger et al. [4] presented theoretical 3D numerical modelling by using the finite element analysis. They found that with high risk of rupture the WSS of the AAA wall is considered as a superior forecaster of higher WSS regions than the AAA diameter. Furthermore, Deplano et al. [3] conveyed that the core of the vortices inside AAA inflatable similar are extremely reliant on the blood flow wavy forms. The impacts of the vortices between them can increase the local pressure happening on the walls of the AAA and this process will lead to increase the local WSS.

Some aorta models were simulated numerically with a pulsatile inlet waves for both the resting and exercise conditions. Lee and Chen [13] presented the velocity vectors, iso-velocity contours, WSS distribution, and the recirculation zones. Thus, the flow behaviour and vortices impacts the AAA wall acting a significant role in the rupture mechanism. Therefore, the main objective of the present paper is to analyse the effects of using Newtonian and non-Newtonian blood flow, WSS variation inside the AAA, secondary blood flow patterns, flow separations localization and vortices regions, on the instruction between the presence of saccular AAA and arterial bifurcation.

2. Problem formulation

2.1. Clinical anatomy and physical domain

The artery called the abdominal aorta, when the aorta enters the abdomen. From its beginning until its end, the abdominal aorta supplies five main vascular branches by the two iliac arteries bifurcation abdominal aorta and the bifurcation into the Left Iliac Arteries (LIA) and Right Iliac Arteries (RIA) [10]. This model comprises a normal aorta approximately 1.9 to 2.2 cm in

diameter [11], but when it reaches to the abdominal aorta region its diameter becomes about 0.9 cm, while AAA as large as 1.7 cm in diameter, as shown in Fig. 1 [5, 18].

Fig. 1 Clinical case of 73-year-old male patient with AAA [17]

After the dimensions of the abdominal aorta with aneurysm and bifurcation were determined from the image, a model of the geometry was designed using CAD software with aid of Gambit program. Finally, it was exporting and simulating by the ANSYS-Fluent 15.0 [6]. The physical domain for the two cases have employed in this study is plotted in Fig. 2.

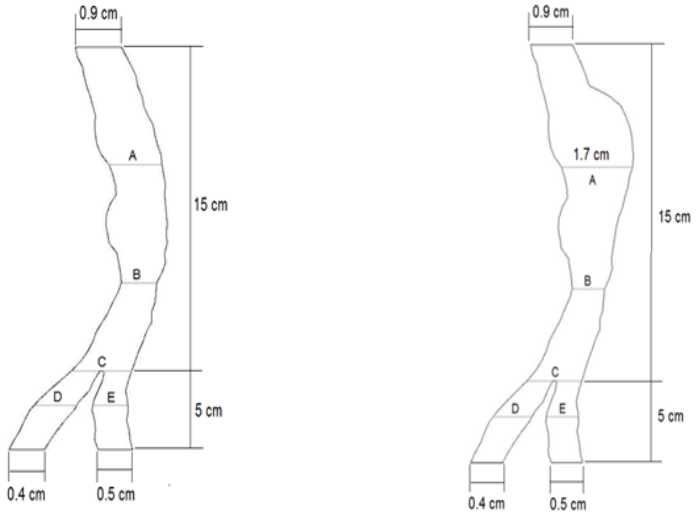

a) without FAAA b) with FAAA

Fig. 2 Real problem geometry of the present work for with and without FAAA models

2.2. Mathematical model

In small arteries or capillaries, the blood displays non-Newtonian fluid properties only, but if the blood flows in large vessels the blood can be model as a Newtonian fluid fung [7]. In this study, blood has assumed incompressible, homogeneous, Newtonian, and non-Newtonian blood fluid. The flow of the blood is demonstrated to be unsteady, laminar, two-dimensional, and fully developed flow. Blood is characterized by generalized Carreau model non-Newtonian model. Under these assumptions ANSYS-Fluent 15.0 was used to solve the governing equations that may be written by using the Navier-Stokes equations that given as follow [6]:

The continuity equation:

$$u\nabla u = 0, \tag{1}$$

r-component of momentum equation:

$$\rho\left(\frac{\partial u}{\partial t}+u\nabla u\right)=-\nabla p_r+\nabla\Gamma, \tag{2}$$

x-component of momentum equation:

$$\rho\left(\frac{\partial v}{\partial t}+v\nabla v\right)=-\nabla p_y+\nabla\Gamma, \tag{3}$$

where Γ represens the tensor of stress that is directly proportional of the deformation rate tensor *D* as:

$$\Gamma=2\eta(\dot{\gamma})D, \tag{4}$$

$$D=\frac{1}{2}\left(\nabla u+\nabla u^{\mathrm{T}}\right). \tag{5}$$

For a Newtonian blood fluid assumption η is assumed as a constant, but for a non-Newtonian blood fluid assumption η is supposed as a function of the shear rate γ. It can be modelled by using Carreau model as:

$$\mu(\dot{\gamma})=\mu_\infty+\frac{\mu_0+\mu_\infty}{\left(1+\left(m\dot{\gamma}\right)^2\right)^{\frac{1-n}{2}}}. \tag{6}$$

The thermo-physical properties and rheological parameters of the Newtonian and non-Newtonian blood model used in the present numerical calculation are listed in the Table 1.

Table 1. Measured properties of human whole blood at 37 °C [4]

Properties	**Value**	**Unit**
Density, (ρ)	1060	kg/m^3
Specific heat, (C_p)	4128	J/kg·K
Thermal conductivity, (k)	0.542	W/m·K
Relaxation factor, (β)	0.0035	1/K
Dynamic viscosity, (μ)	0.0037	Pa·s
Zeros dynamic viscosity, (μ_0)	0.056	Pa·s
Infinity dynamic viscosity, (μ_∞)	0.0345	Pa·s
Consistency coefficient, (m)	3.313	Pa·sn
Flow behavior index, (n)	0.3568	-

Blood is related to its microscopic structures for shear thinning non-Newtonian model and it is determined mainly by aggregation, deformation and alignment of red blood cells [17]. The shear thinning model is the prevailing the non-Newtonian blood fluid property that disturbing the velocity [8]. Also, the turbulent flow can be modelled by using many modelling of turbulence schemes such as the *k*-ε two-equations:

k-turbulent kinetic energy equation is written as:

$$\frac{1}{r}\left\{\frac{\partial}{\partial x}(\rho ruk)+\frac{\partial}{\partial r}(\rho rvk)\right\}=\frac{1}{r}\left\{\frac{1}{r}\frac{\partial}{\partial x}\left(r\frac{\mu_{eff}}{\sigma_k}\frac{\partial k}{\partial x}\right)+\frac{\partial}{\partial r}\left(r\frac{\mu_{eff}}{\sigma_k}\frac{\partial k}{\partial r}\right)\right\}+S_k\,, \tag{7}$$

ε-dissipation rate of turbulent kinetic energy equation is written as:

$$\frac{1}{r}\left\{\frac{\partial}{\partial x}(\rho ru\varepsilon)+\frac{\partial}{\partial r}(\rho rv\varepsilon)\right\}=\frac{1}{r}\left\{\frac{1}{r}\frac{\partial}{\partial x}\left(r\frac{\mu_{eff}}{\sigma_\varepsilon}\frac{\partial \varepsilon}{\partial x}\right)+\frac{\partial}{\partial r}\left(r\frac{\mu_{eff}}{\sigma_\varepsilon}\frac{\partial \varepsilon}{\partial r}\right)\right\}+S_\varepsilon\,, \tag{8}$$

where

$$S_k=G+C_D\rho\varepsilon\,, \tag{9}$$

$$S_\varepsilon=\frac{\varepsilon}{k}\left(C_1G+C_2\rho\varepsilon\right), \tag{10}$$

$$G=\mu_t\left\{2\left[\left(\frac{\partial u}{\partial x}\right)^2+\left(\frac{\partial v}{\partial r}\right)^2+\left(\frac{v}{r}\right)^2\right]+\left(\frac{\partial u}{\partial r}+\frac{\partial v}{\partial x}\right)^2\right\}-\frac{2}{3}\mu_t\left[\frac{1}{r}\frac{\partial}{\partial r}(rv)+\frac{\partial u}{\partial x}\right]^2. \tag{11}$$

Here, C_1, C_2, σ_k and σ_ε represent the empirical turbulence constants. The recommended values are given in Table 2 [5].

Table 2. Empirical constants in *k*-ε model [5]

C_1	C_2	σ_k	σ_ε	C_μ	C_D	I	λ
1.44	1.92	1.0	1.314	0.5478	0.1634	0.03	0.005

2.3. Boundary conditions

Boundary conditions defined in this paper as shown in Fig. 3 are as following: at the entrance of the artery wall model, there is no radial blood flow; thus axial velocity slope may be supposed to be zero, but the inlet velocity is assumed as a constant at value considered in [9] at the entrance of the aorta (u_0 = 20 cm/s); for laminar flow there is no shear rate of blood fluid flow sideways of the axis. At artery wall, it is assumed that the no slip condition must be used along the artery walls, thus the blood velocity is taken at zero on the artery walls. In the exit of the artery wall model, the pressure at the exit is set to 0 Pa. As the initial condition, it is supposed that there is no flow happing when the model system is at rest (t = 0 s).

2.4 Numerical simulation

In this study, the artery geometry was drawn by Gambit program. It is employed to arrange the computational domain geometry and to build the grid model to analyse the problems as show in Fig. 4. In order to simulate the classic single-phase shear thinning behaviour of the blood and Newtonian fluid two new "materials" have created in the ANSYS-Fluent in the fluids database. The first one that simulates the blood is non-Newtonian and follows a Carreau model, Eq. (7). The second one is Newtonian with constant viscosity at 3.5 cP. The problem of using the real geometry of irregular artery wall of arterial bifurcation model with AAA has simulated by ANSYS-Fluent 15.0 CFD program, due to the complexity of the present abdominal aorta wall.

According to the finite volume technique, the system governing equations are solved consecutively by segregated one another.

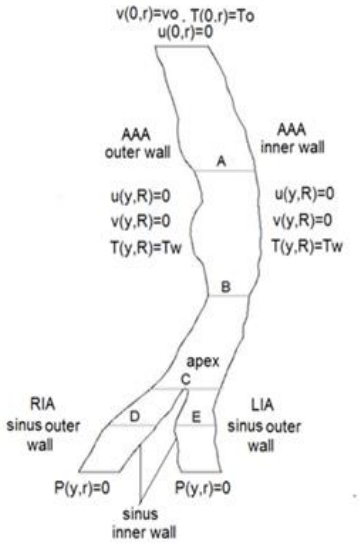

Fig. 3 Real problem geometry

The Semi Implicit Method for Pressure Linked Equations (SIMPLE) was utilized to couples the pressure and velocity effects solution [17]. The criterion of the convergence for velocity is less than 1.0×10^{-5}, and the criterion for temperature is less than 1.0×10^{-6}. Results of velocity distribution at the bifurcation for Reynolds number 410 was compared for four different grids. The solution sizes of grid numbers were selected as:

- Without AAA (WAAA): nodes = 105098, 103869 quadrilateral cells, all 103 edges with interval size of 0.5, for 1 faces-elements of Quad type and Pave, the maximum number of iteration for Newtonian = 490 and non-Newtonian = 370;
- With AAA (AAA): nodes = 206510, 204560 quadrilateral cells, all 121 edges interval size of 0.6, for 1 faces-elements of Quad type and Pave, the maximum number of iteration for Newtonian = 620, non-Newtonian = 480.

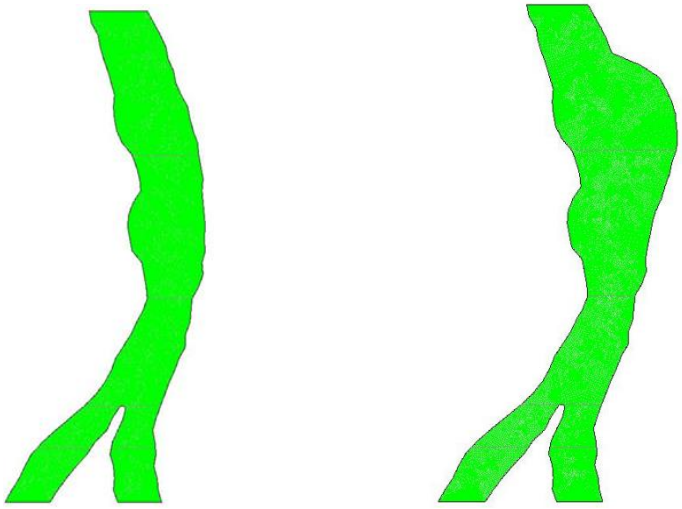

a) without FAAA b) with FAAA

Fig. 4 Solution computational domain and grid generated used in the present analysis

3. Results and discussion

In the following text, some of observations and comments made that assumed from results gotten from extensive ranges of blood flow conditions and numerical simulation are presented. In order to give indication for the blood flow profile in semi-realistic aneurysms AAA, it is necessary straightforward to sense the flow patterns by extrapolating from knowledge gained from idealized models alone.

3.1. Flow field

Numerical simulations for two models of abdominal aorta for with and without AAA have used to find the effect of presence of the AAA on the flow field and heat transfer in abdominal and arterial perfection for Reynolds number, Re = 410. The blood in two cases was Newtonian and non-Newtonian. Fig. 5 shows the pressure magnitudes approximating along an abdominal aorta with AAA (position A, according Fig. 3) compared with case of without AAA. It is shown that the presence of AAA in the flow direction caused to decreasing the peak pressure (position A) and pressure distribution in the aorta. However, it will increasing the stagnation pressure in the region of starting the bifurcation. The effect of using non-Newtonian blood model illustrated in Fig. 6.

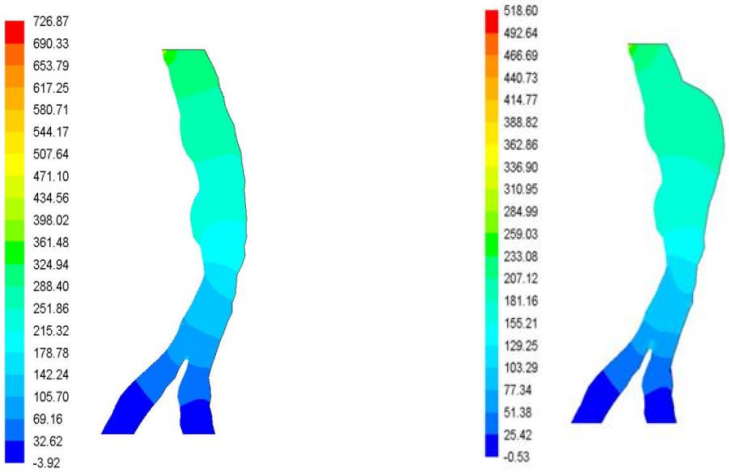

a) without FAAA b) with FAAA

Fig. 5 Newtonian blood contour of static pressures laminar flow (Re = 420)

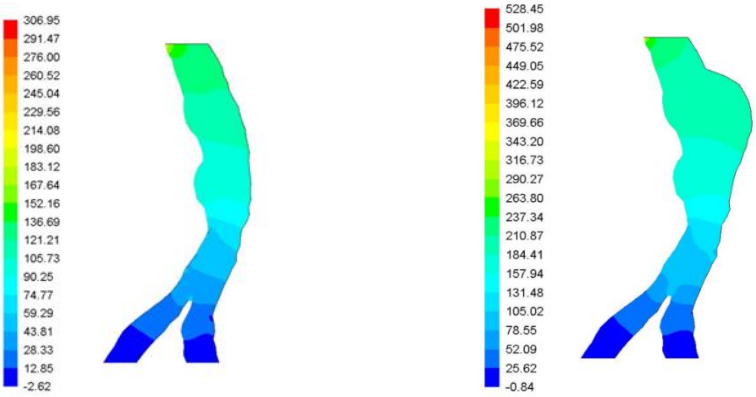

a) without FAAA b) with FAAA

Fig. 6 Non-Newtonian blood contour of static pressures laminar flow (Re = 420)

The effect of AAA on the velocity contour is presented in Figs. 7 and 8 for Newtonian and non-Newtonian blood model for laminar flow at Re = 420. Clearly, we can observe that the velocity magnitude in AAA inner wall region (position A) due to increase the cross section area and this will lead to dramatically increase the inner pressure that applies on the inner AAA wall and then increasing the probability of the AAA rapture. But, as compared Fig. 7b and Fig. 8b, it is shown that the blood velocity decreased in AAA region (position A), but the blood velocity increased in the construction region (position B, according Fig. 3) of the abdominal region for all flow conditions.

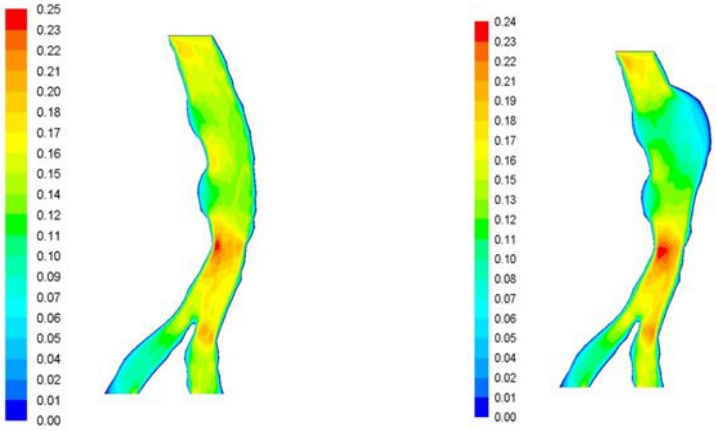

a) Without FAAA b) With FAAA

Fig. 7 Newtonian blood velocity counter in (m/s) laminar flow (Re = 420)

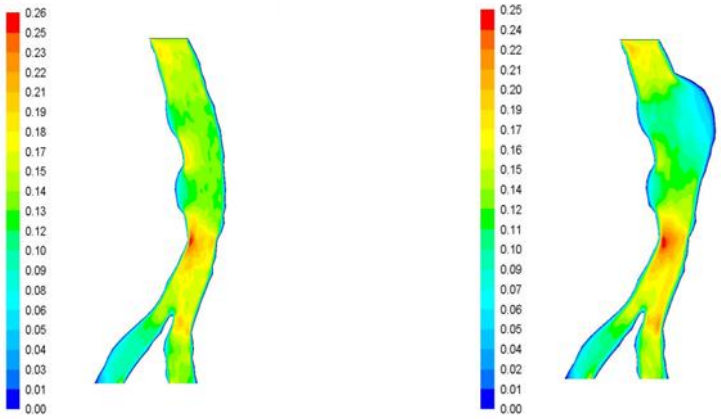

a) without FAAA b) with FAAA

Fig. 8 Non-Newtonian blood velocity in (m/s) laminar flow (Re = 420)

The axial velocity vector in plane of bifurcation is presented in Fig. 9. The effect of AAA on velocity vector of Newtonian and non-Newtonian models of the blood flows at Re = 2500 is shown. If compared between Fig. 9a and Fig. 9b, we show that the using non-Newtonian power law blood model will give a same flow pattern. The results show that as the flow accelerates to the peak point that near AAA inner wall (position A), recirculation vortex grew slightly stronger. This causing negative velocity gradients and increasing the recirculation regions size. However, in the branching region of the aorta it is shown that generation a secondary flow motion in the vessel curvature introduces radial pressure gradient from the outside wall towards the apex. The size of the secondary vortex pair that produced depends on the curvature radius, diameter of vessel, and flow velocity. In addition, in the bifurcation region (positions C and D, according Fig. 3) show that the blood velocity profiles were skewed towards the apex.

In the region along the outer ICA wall, it is shown that the development of the low momentum can clearly be seen and spans approximately 50% of the sinus volume at mid sinus (position B).

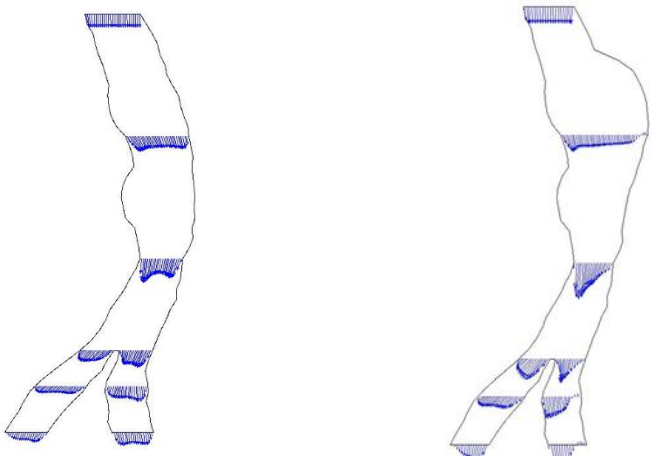

a) without FAAA b) with FAAA

Fig. 9 Non-Newtonian blood velocity counter turbulent flow

The effects of presence the AAA on velocity vector can be shown in Fig. 10. It is shown that the reversed flow clearly in the inner region of the AAA due to increase the area of blood vessel and decreased both the pressure and momentum in this region. The blood velocity vectors are no longer parallel in the region just beyond the AAA. But, in a separation flow region at the condition of the blood laminar flow is greatest concerned just beyond the tapering of the blood vessel. In the region inside the AAA, the results shown that there is a separation region in flow stream that is located near the bulge region when the velocities are low and flow reversal happened.

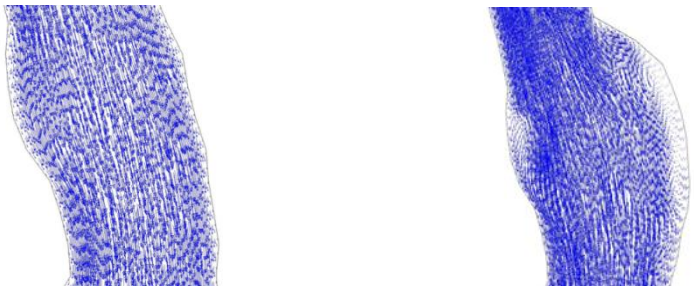

a) without FAAA b) with FAAA

Fig. 10 Newtonian blood velocity vector turbulent flow in the AAA region

3.2. Vortex dynamics

For more visualization the flow field using the velocity stream along the entire computational domain is shown on Fig. 11. It is shown the increase of the Reynolds number for the case without AAA. The flow pattern did not change significantly as illustrated Fig. 11a for AAA inner wall region (position A).

3.3. Artery static pressure

Fig. 12 plotted four positions along path of fluid flow of y/L = 0.25, 0.55, 0.75, 0.85 and 0.85. It is shown that pressure reduced with increase of r/D (Fig. 12a, position A) of y/L = 0.25 for without AAA. If consider the case of with AAA, the pressure will increase with the increase of r/D (Fig. 12b) for same laminar flow condition. The construction region of the artery in position

B is plotted in Fig. 12b. It is shown that the pressure increased with increasing of *r/D* for the two cases and increased from 0.61 to 0.66 at *r/D* = 0.9 when using the model of AAA for laminar flow. Nevertheless, when the Re rose from 410 to 2500 the pressure raised from 0.4 to 0.65 when using model of AAA for turbulent flow. The pressure profile in the arterial bifurcation entrance (when the artery parent divided into two daughter right and left) in section of position C is plotted in Fig. 12c. It is found that the static pressure show a peak value in the stagnation point of the bifurcation region, due to the zeros velocity in this point and conversion all the convective force into pressure force as the flow will be impact this point. The RIA (position D) is plotted in Fig. 12d. The static pressures will increase with *r/D* for the two cases of with and without AAA value in this region, but the AAA model will give the highest values.

a) without FAAA b) with FAAA

Fig. 11 Newtonian blood velocity streamline laminar flow (Re = 420) in the AAA region

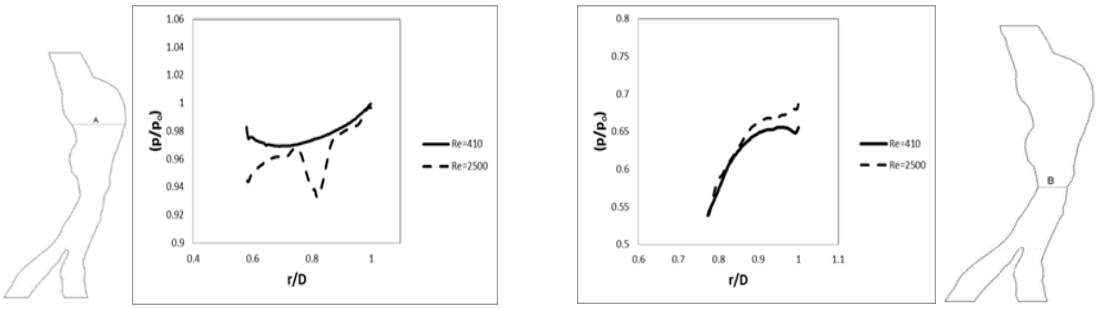

a) Position A, *y/L* = 0.25 b) Position B, *y/L* = 0.55

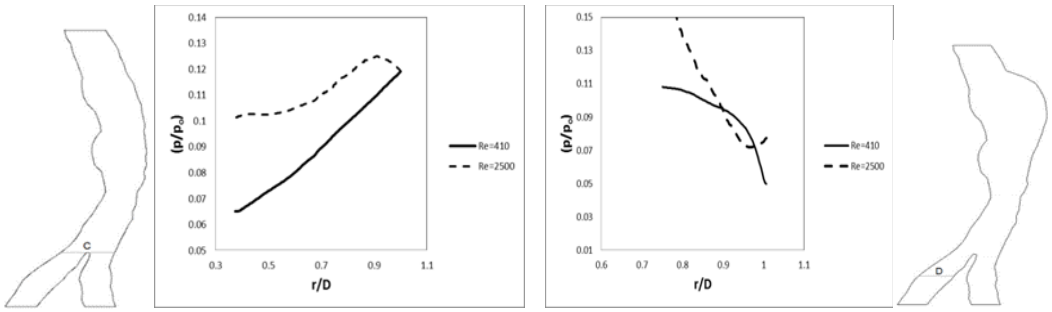

c) Position C, *y/L* = 0.75 d) Position D, *y/L* = 0.85

Fig. 12 Normalized pressure (*P/Po*) verse dimensionless radial artery distance of with AAA case Newtonian blood

Moreover, to study the effects of AAA on dimensionless velocity (v/v_o) in *y*-direction for laminar and turbulent Newtonian blood model for four positions is presented in Fig. 13. The velocity data are normalized with respect to the maximum velocity. However, the figures

show that the general profile would change from position to anther due to changing the inner diameters of the artery vessel along blood flow bath in *y*-direction. In this study a real geometry of the vessel for irregular boundary wall of the artery is used. In addition, this gave a good indicator of the real picture of the hemodynamics of blood flow in realistic abdominal artery. It is shown that the velocity reduced from v/v_o = 1.15 for without AAA to 0.87 by 24% for with AAA at middle position of the flow at r/D = 0.8. However, the dimensionless velocity reduced from v/v_o = 0.85 for without AAA to 0.37 by 56% for with-AAA at r/D = 1.0 at inner wall of the AAA as shown in Fig. 13a for artery section of y/L = 0.25 (position A). The turbulent flow model will cause to reduce the velocity too, but with high value as compared Fig. 13b. It is shown that the velocity reduced with blunt profile across the section of artery and is increased near the wall with 28% and 59% percent for middle and region, respectively. By forward to construction region of artery (position B) at y/L = 0.55 compared between the two cases of without and with AAA is presented in Fig. 13c. It is observed that the reduction in artery diameter will cause increasing the velocity of laminar and turbulent flow condition with fluctuation flatter profile for turbulent case. The dimensionless velocity profile in the entrance of arterial bifurcation (position C) is presented in Fig. 13d. It is shown that there are three positions of the zeroes velocity instead of two due to the point of stagnation pressure in the apex point.

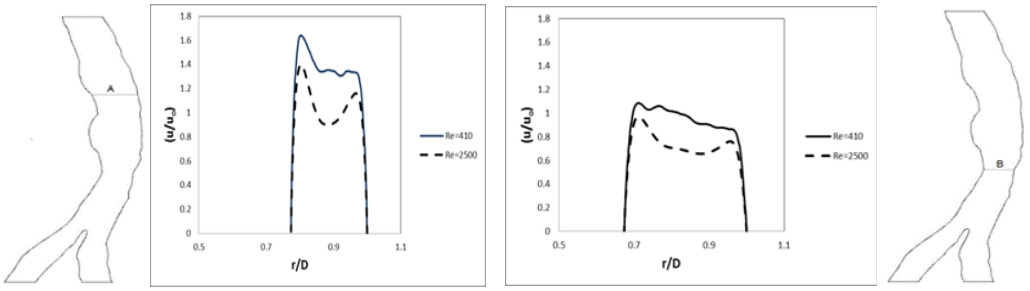

a) Position A, y/L = 0.25 b) Position B, y/L = 0.55

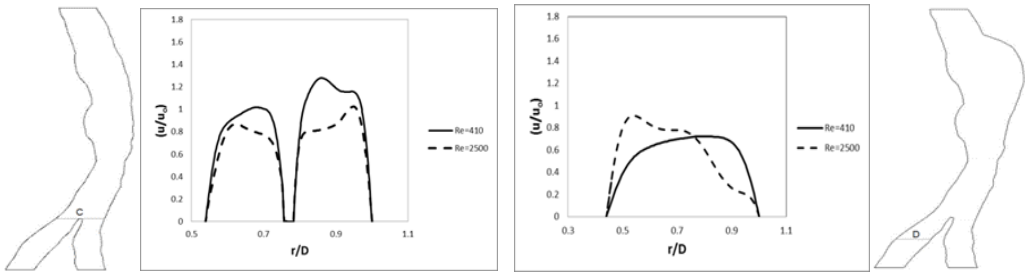

c) Position C, y/L = 0.75 d) Position D, y/L = 0.85

Fig. 13 Normalized stream velocity (v/v_o) verse radial artery distance of without AAA case

3.4. Study aneurysm region

The main purpose of this work was to examine the outcome of unsymmetrical irregular wall aneurysm on the blood hemodynamics in the abdominal and arterial bifurcation. In order to increase the focus on the aneurysm regions, it was used eight sections in the two cases of with and without AAA to plot the pressure, velocity and temperature distribution. Fig. 14 shows that the present aneurysm would effect on the increasing the pressure on the inner wall of the AAA and increasing the velocity blunt profiler as compared with and without AAA in Fig. 14a. Generally, the static pressure decreased in case of with AAA due to increase the cross section area of the flow and increased the radial distance of the AAA region. Fig. 14b presented the numerical data of the velocity in eight sections of the AAA region. It is shown that the presence

of AAA will cause to increase the velocity in the distal (section 1, Fig. 14) of the AAA and then decreased gradually near the inner wall of the AAA with increased the radial distance of the artery aneurysm region.

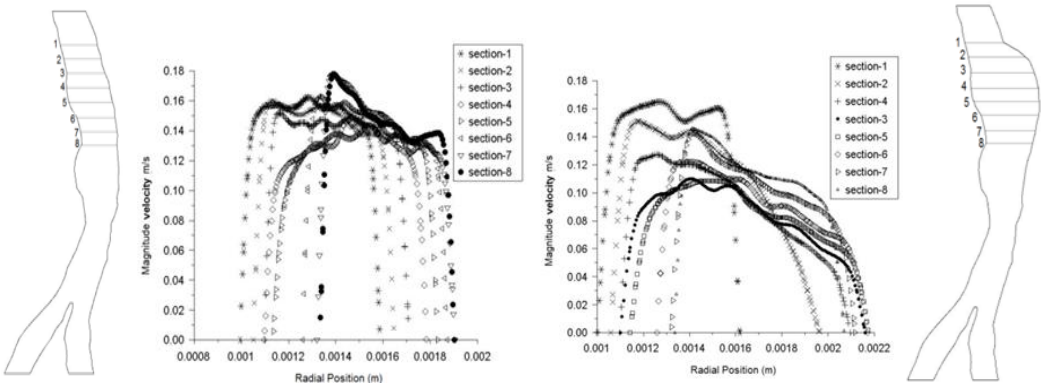

a) without FAAA b) with FAAA

Fig. 14 Aneurysm regions using eight section in case of with and without AAA, Re = 410

Fig. 15 performed the possessions of the turbulent flow on hemodynamics blood flow field of blood in the AAA region. It is shown that the presence of aneurysm leads to increasing the static pressure on the inner wall of the AAA with fluctuating profile and reversed flow in low momentum of separation near the inner wall of AAA as shown in Fig. 15a. It is illustrated velocity along radial distance of artery in developing aneurysm region. It is presented the numerical data of the velocity in eight sections of the AAA regions.

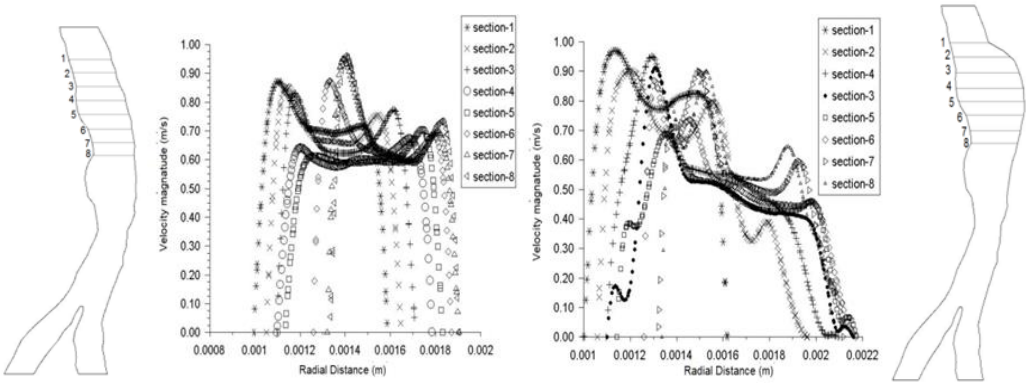

a) without FAAA b) with FAAA

Fig. 15 Aneurysm regions using eight section in case of with and without AAA, Re = 2500

3.5. Wall shear stress

The study of the WSS plays a significant role in the hemodynamics in the resent years. Thus, the shear stresses along the artery wall for blood Reynolds number of Re = 410 for two wall boundary of AAA and sinus inner wall as plotted in Figs. 16 and 17. In general, it is observed that a fluctuation profile along the AAA inner wall due to the irregularity of the artery wall boundary. In addition, it is important to mention that the calculated WSS from the CFD simulations were compared between the Newtonian (Fig. 16) and Careaue model for non-Newtonian blood (Fig. 17). It shows that the WSS increases by 33% for using the Newtonian blood model at y/L = 0.4 in region of abdominal aorta which extended from y/L = 0 to 0.75 at Re = 410. When the blood flow interned the arterial bifurcation region that extending from y/L = 0.75 to 1.0, it is shown that the WSS fluctuating and increased gradually until it

reaches the peak value in turbulent flow of WSS = 600 Pa particular at *y/L* = 0.87. As it is obvious, there is a good agreement between simulations of the wall shear stress results for both the Newtonian and the non-Newtonian fluids. In addition, it is cleared that the shear stresses on sinus inner wall along arterial bifurcation are having the fluctuating profile but with lower value than these on the AAA inner wall that along abdominal aorta. Moreover, it is gave high shouted increasing in the middle position of the bifurcation. The Newtonian increased by 25% than the non-Newtonian at *y/L* = 0.93.

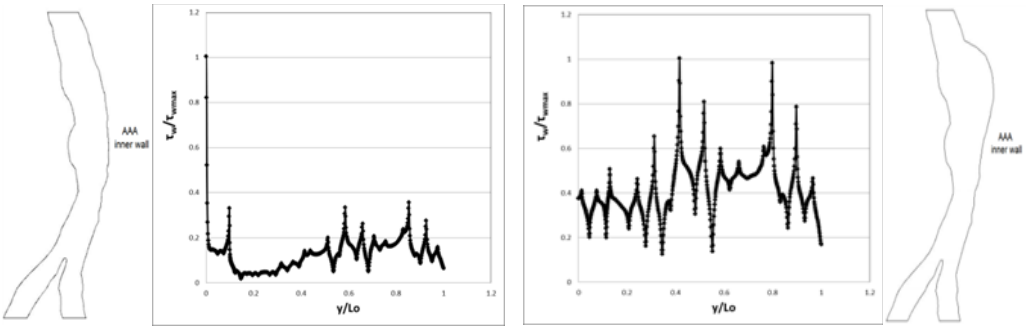

a) without FAAA b) with FAAA

Fig. 16 Newtonian WSS verse the dimensionless axial artery distance (*y/L*)

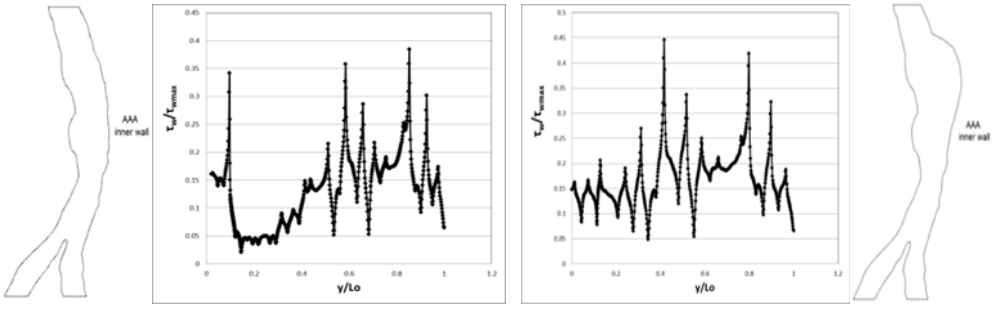

a) without FAAA b) with FAAA

Fig. 17 Non-Newtonian WSS verse the dimensionless axial artery distance (*y/L*)

3.6. Numerical model validation

The investigated areas were the abdominal aorta with AAA and the two iliac arteries of the right and left branches. The computer simulation data are well fitted on those obtained by *in vitro* experimental by Yu [20] that works by PIV as presented in Fig. 18.

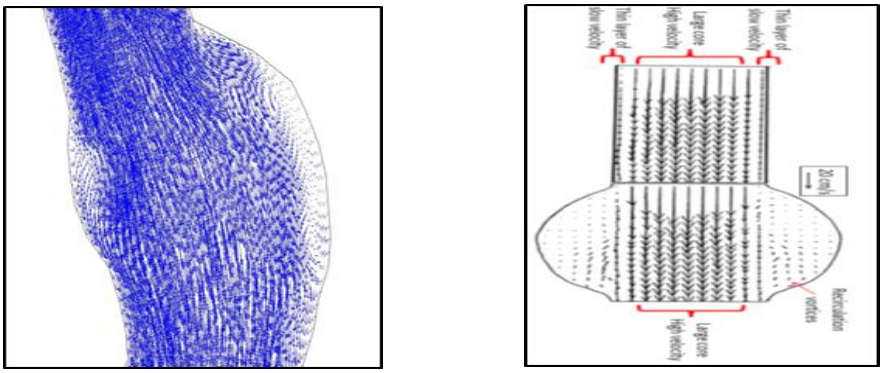

a) Present work b) Yu work, [20]

Fig. 18. Validation the present numerical results of velocity vector field at the same velocity about 20 cm/s with the experimental of Yu work, [20]

Fig. 18 shows that the blood velocity measured values obtained by experimental works of Yu [20] ranges from 20-23 cm/s, but the range 20-22 cm/s in the domain along the main flow path lines of the velocity value obtained by present simulation. A comparison between the present simulations with the PIV experimental results of velocity vector for steady flow condition that given by Yu [20] were considered in order to validate blood flow modelling approach. It shows that there is a coincident of the two results, where there are three regions: 1) zero velocity near wall in the entry of AAA; 2) large convicted middle region of artery in the entry of AAA and 3) vortices region along inner wall region of AAA for these works.

Conclusion

The numerical results of the laminar and turbulent flow, Newtonian and non-Newtonian fluid blood model, with and without AAA in abdominal aorta, were investigated in this study in order to consider the importance of turbulent blood flow to evaluate the hemodynamic parameters. The results show that the AAA hemodynamic patterns depend on wall configuration of the AAA boundary geometric. The data for the 2D reconstruction of the numerical simulation show that at the turbulent flow, the velocity with highest fluctuation profile and generation of some vortices near the inner wall of AAA are observed. The highest values of WSS levels obtained downstream of AAA and at bifurcation apex are shown. The presence of AAA in flow path will increase blood velocity of the distal by 35% for laminar and about 42% for turbulent. Finally, the present approach for modelling was validated by comparison with the previous corresponding experimental velocity patterns results and gave a respectable agreement between the present simulation results and this experimental work.

References

1. Altuwaijri O. (2012). Advanced Computer Modeling of Abdominal Aortic Aneurysms to Predict Risk of Rupture, PhD Thesis, University of Hull, England.
2. Cowan J. A. Jr., J. B. Dimick, P. K. Henke, J. Rectenwald, J. C. Stanley, G. R. Upchurch Jr. (2006). Epidemiology of Aortic Aneurysm Repair in the United States from 1993 to 2003, Ann N Y Acad Sci, 1085, 1-10.
3. Deplano V., Y. Knapp, E. Bertrand, E. Gaillard (2007). Flow Behaviour in an Asymmetric Compliant Experimental Model for Abdominal Aortic Aneurysm, J Biomech, 40, 2406-2413.
4. Fillinger M., F. Marra, P. Raghavan, E. Kennedy (2003). Prediction of Rupture Risk in Abdominal Aortic Aneurysm during Observation: Wall Stress versus Diameter, J Vasc Surg, 37, 724-732.
5. Finol E. A., C. H. Amon (2001). Blood Flow in Abdominal Aortic Aneurysms: Pulsatile Flow Hemodynamics, J Biomech Eng, 123(5), 474-484.
6. Fluent Release 6.2.16, Fluent Incorporated, March 7, 2005, Lebanon, NH, USA.
7. Fung Y. C. (1993). Biomechanics: Mechanical Properties of Living Tissues, Springer-Verlag New York.
8. Gijsen F. J., F. N. Van deVosse, J. D. Janssen (1999). The Influence of the Non-Newtonian Properties of Blood on the Flow in Large Arteries: Unsteady Flow in a 901 Curved Tube, J Biomech, 32, 705-713.
9. Gosman A. D., F. K. Ideriah (1983). TEACH-2E: A General Computer Program for Two-dimensional Turbulent Recirculating Flows, International Report, Department of Mechanical Engineering Imperial College, University of London.
10. Gray H. (1918). Anatomy of the Human Body, Philadelphia, Lea & Febiger.
11. Imray C. (2006). Managing an Abdominal Aortic Aneurysm, Practical Cardiovascular Risk Management, 4, 9-11.

12. Karkos C., U. Mukhopadhyay, I. Papakostas, J. Ghosh, G. Thomson, R. Hughes (2000). Abdominal Aortic Aneurysm: The Role of Clinical Examination and Opportunistic Detection, Eur J Vasc Endovasc Surg, 19(3), 299-303.
13. Lee D., J. Y. Chen (2003). Pulsatile Flow Fields in a Model of Abdominal Aorta with Its Peripheral Branches, Biomed Eng: Appl Basis Commun, 15(05), 170-178.
14. Molla M. (2009). LES of Pulsatile Flow in the Models of Arterial Stenosis and Aneurysm, PhD Thesis, University of Glasgow.
15. Peattie R. A., T. J. Riehle, E. I. Bluth (2004). Pulsatile Flow in Fusiform Models of Abdoiminal Aortic Aneurysms: Flow Fields, Velocity Patterns and Flow-induced Wall Stresses, J Biomech Eng, 126(4), 438-446.
16. Speelman L., A. Bohra, E. M. Bosboom, G. W. Schurink, F. N. Van de Vosse, M. S. Makaorun, D. A. Vorp (2007). Effects of Wall Calcifications in Patient-specific Wall Stress Analyses of Abdominal Aortic Aneurysms, J Biomech Eng, 129(1), 105-109.
17. Thurston G. B. (1979). Rheological Parameters for the Viscosity, Viscoelasticity and Thixotropy of Blood, Biorheology, 16, 149-162.
18. Uflacker R., J. Robison (2001). Endovascular Treatment of Abdominal Aortic Aneurysms: A Review, Eur Radiol, 11(5), 739-753.
19. Walsh P. W., S. Chin-Quee, J. E. Moore Jr. (2003). Flow Changes in the Aorta Associated with the Deployment of AAAA Stent Graft, Med Eng Phys, 25(4), 299-307.
20. Yu S. C. M. (2000). Steady and Pulsatile Flow Studies in Abdominal Aortic Aneurysm Models Using Particle Image Velocimetry, Int J Heat and Fluid Flow, 21, 74-83.
21. Yu S. C., W. K. Chan, B. T. Ng, L. P. Chua (1999). A Numerical Investigation on the Steady and Pulsatile Flow Characteristics in Axi-symmetric Abdominal Aortic Aneurysm Models with Some Experimental Evaluation, J Med Eng Technol, 23(6), 228-239.

Nomenclatures

C_p specific heat, (J/kg·K)
D inner diameter of the abdominal aorta, (m)
k turbulent kinetic energy, $(m/s)^3$
L axial length, (m)
p fluid static pressure, (Pa)
Re Reynolds number, (Du/v)
r radial coordinate measured from the model symmetry axis
Γ stress tensor
t time, (s)
u_o bulk inlet axial velocity, (m/s)
u velocity component in x-direction, (m/s)
v velocity component in r-direction, (m/s)
x axial distance along pipe, (m)

Greek letter

μ dynamic viscosity, (Pa·s)
γ shear rate, (s^{-1})
η viscosity of the blood
μ_{eff} effective viscosity, (Pa·s)
∇ difference or gradient
ε dissipation rate of turbulent kinetic energy, (m^2/s^3)
ρ density, (kg/m^3)
υ kinematic viscosity, (m^2/s)

Assist. Prof. Kadhum Audaa Jehhef, Ph.D.
E-mail: kadhumaudaa@gmail.com

Assist. Prof. Kadhum Audaa Jehhef has B.Sc., H.Dp., M.Sc., and Ph.D. in Thermal Engineering from Mechanical Engineering Department, University of Technology, Baghdad, Iraq. Kadhum Audaa currently works at the Department of Machines and Equipment, Institute of Technology, Middle Technical University, Baghdad, Iraq. He has more than 10 years of experience in mechanical design using SolidWorks and ANSYS Workbench. He has good experience in ANSYS CFX and Fluent solvers.

Ali Jalal Ali, Ph.D. Student
E-mail: 10678@uotechnology.edu.iq

Ali Jalal Ali is a Ph.D. student in Technology and Methods of Nano Products Manufacturing, Tambov, Russian Federation. Ali had a M.Sc. degree in Thermal Energy and Process Engineering from Belgorod State Technical University, Russian Federation. He currently works at the Biomedical Engineering Department, University of Technology, Baghdad, Iraq. Ali runs research in nanotechnology, mechanical engineering, and biomedical engineering.